

Metal-insulator transition in the dimerized organic conductor κ -(BEDT-TTF)₂Hg(SCN)₂BrTomislav Ivek,^{1,2} Rebecca Beyer,¹ Sabuhi Badalov,¹ Matija Čulo,² Silvia Tomić,² John A. Schlueter,³ Elena I. Zhilyaeva,⁴ Rimma N. Lyubovskaya,⁴ and Martin Dressel¹¹*Physikalisches Institut, Universität Stuttgart, Pfaffenwaldring 57, 70550 Stuttgart, Germany*²*Institut za fiziku, P.O. Box 304, HR-10001 Zagreb, Croatia*³*Division of Materials Research, National Science Foundation, Arlington, VA 22230, and Material Science Division, Argonne National Laboratory, Argonne, Illinois 60439-4831, USA*⁴*Institute of Problems of Chemical Physics, Russian Academy of Sciences, RU-142 432 Chernogolovka, Moscow oblast, Russia*

(Received 13 June 2017; published 10 August 2017)

The organic charge-transfer salt κ -(BEDT-TTF)₂Hg(SCN)₂Br is a quasi-two-dimensional metal with a half-filled conduction band at ambient conditions. When cooled below $T = 80$ K, it undergoes a pronounced transition to an insulating phase where the resistivity increases many orders of magnitude. In order to elucidate the nature of this metal-insulator transition, we have performed comprehensive transport, dielectric and optical investigations. The findings are compared with other dimerized κ -(BEDT-TTF) salts, in particular the Cl analog, where a charge-order transition takes place at $T_{CO} = 30$ K.

DOI: 10.1103/PhysRevB.96.085116

I. INTRODUCTION

The current interest in dimerized two-dimensional organic conductors mainly focusses on κ -(BEDT-TTF)₂X salts built with extended polymeric anions X^- such as $\text{Cu}(\text{SCN})_2^-$, $\text{Cu}[\text{N}(\text{CN})_2]\text{Br}^-$, $\text{Cu}[\text{N}(\text{CN})_2]\text{Cl}^-$, or $\text{Cu}_2(\text{CN})_3^-$, all containing copper ions. These systems are characterized by half-filled conduction bands and are located in proximity to correlated insulating states. Depending on the strength of the on-site Coulomb repulsion U with respect to the bandwidth W , a metallic and superconducting ground state develops at low temperatures, or a Mott insulator, which might be antiferromagnetically ordered or behaves like a spin liquid due to strong frustrations [1–3].

Subsequent theoretical approaches [4–7] suggest that also the Coulomb interaction V between the dimers has to be included in the description of possible charge-ordering phenomena in these dimerized (BEDT-TTF) salts. Although numerous experimental results [8–13], rule out appreciable charge disproportionation in κ -(BEDT-TTF)₂Cu [N(CN)₂Cl_x], κ -(BEDT-TTF)₂Cu₂(CN)₃ and other copper-based κ -(BEDT-TTF)₂X salts, these considerations might be relevant for dimerized salts in general. Unfortunately, charge-order phenomena in κ -phase salts with an effectively half-filled band are scarce and only a few compounds are reported exhibiting charge order, such as κ -(BEDT-TTF)₄PtCl₆ · C₆H₅CN, the triclinic κ -(BEDT-TTF)₄[M(CN)₆][N(C₂H₅)₄] · 3H₂O and the monoclinic κ -(BEDT-TTF)₄[M(CN)₆][N(C₂H₅)₄] · 2H₂O (with $M = \text{Co}^{\text{III}}$, Fe^{III} , and Cr^{III}) salts [14]. Here the structure is rather complex as the phase transition includes the deformation of the molecule and the interaction with the anions; accordingly, details of their physical properties and their electronic states are not well known. Certainly, electronic correlations as well as coupling to the lattice are important.

Recently it was demonstrated that κ -(BEDT-TTF)₂Hg(SCN)₂Cl undergoes a pronounced charge order transition at $T_{CO} = 30$ K [15,16], as illustrated in Fig. 1. The insulating state is rapidly suppressed by hydrostatic pressure of $p = 4.2$ kbar without any signs of superconductivity [17]; making this compound distinct from κ -(BEDT-TTF)₂Cu[N(CN)₂Cl], where a tiny amount of

pressure drives the Mott insulator superconducting, but also from the canonical charge-ordered system α -(BEDT-TTF)₂I₃ [18,19]. The present investigation now addresses the question in which way κ -(BEDT-TTF)₂Hg(SCN)₂X is modified when replacing $X = \text{Cl}$ by Br in the anion sheet. Let us recall that in the case of κ -(BEDT-TTF)₂Cu[N(CN)₂Cl] the corresponding substitution pushes the antiferromagnetic Mott insulator into a superconducting phase with $T_c \approx 12$ K [1].

The family of κ -(BEDT-TTF)₂X salts with mercury-based anions have a structure similar to the Cu salts [20], but different ratios of transfer integrals, which result in modified parameters used to map them on the Hubbard model [21]. In particular the orbital overlap t_d within the dimers of the Hg compounds is weaker compared to the Cu family, causing a reduced on-site repulsion U with respect to the interdimer interaction. This makes it necessary to go beyond the simple Hubbard model, which allowed to treat the Cu-based κ -(BEDT-TTF) compounds successfully as half-filled system with one electron per dimer [3,22]. Now the description has to start from individual BEDT-TTF molecules, leading to a quarter-filled conduction band; in addition to U , the intermolecular interaction V has to be included in the extended Hubbard model.

In an effective dipolar-spin model, Hotta suggests [4] that quantum electric dipoles are formed on the dimers, which interact with each other and thus modify the exchange coupling. Since they fluctuate by t_d , for large orbital overlap the dimer Mott insulator is stable, forming a dipolar liquid; if V is large compared to t_d , however, charge order emerges (dipolar solid). Similar considerations have been put forward by other groups [5,6]. Mazumdar, Clay, and collaborators [7] could show that in these system a frustration-induced transition occurs from a Néel antiferromagnetism to a spin-singlet state in the interacting quarter-filled band on an anisotropic triangular lattice. In the spin-singlet state, the charge on the molecules becomes unequal: a paired-electron crystal is formed with pairs of charge-rich sites separated by pairs of charge-poor sites. This spin-singlet formation is driven by quantum effects at any value of nearest-neighbor interaction V .

Here we present the first comprehensive transport, dielectric and optical investigations of κ -(BEDT-TTF)₂Hg(SCN)₂Br and

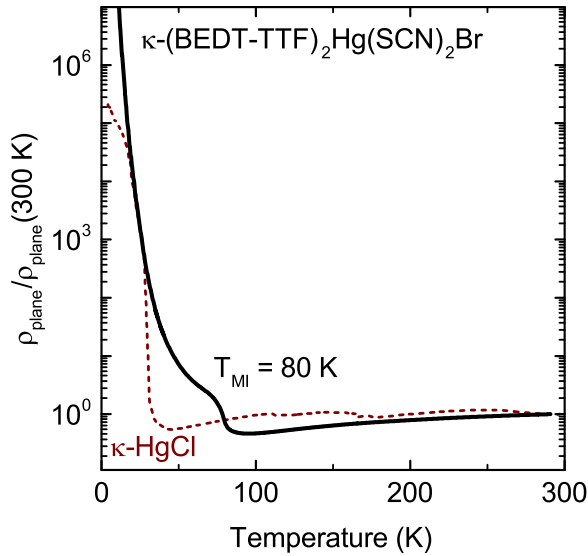


FIG. 1. Temperature dependence of the normalized dc resistivity of κ -(BEDT-TTF) $_2$ Hg(SCN) $_2$ Br measured within the highly conducting (bc) plane. By cooling below $T_{MI} = 80$ K a metal to insulator transition occurs. For comparison, the normalized dc resistivity of sibling compound κ -(BEDT-TTF) $_2$ Hg(SCN) $_2$ Cl is plotted as dashed line; due to charge ordering the system becomes insulating below $T_{CO} = 30$ K.

discuss the findings within the framework of dimerized Mott insulators composed by these Hg and Cu families.

II. EXPERIMENTAL DETAILS

A series of κ -(BEDT-TTF) $_2$ Hg(SCN) $_{3-n}$ X $_n$ salts with $X = \text{F, Br, I}$ ($n = 1$) and $X = \text{Cl}$ ($n = 1, 2$) has been synthesized by Lyubovskii and collaborators already twenty years ago [23,24], ranging from insulators to metals and possible superconductors [20]; a thorough investigation of their physical properties, however, is still lacking. Here we have turned our attention to κ -(BEDT-TTF) $_2$ Hg(SCN) $_2$ Br, an isostructural sister compound of the charge-ordering κ -(BEDT-TTF) $_2$ Hg(SCN) $_2$ Cl; as demonstrated in Fig. 1, it also exhibits a metal-insulator transition upon cooling, but at somewhat higher temperatures.

Based on recent x-ray scattering experiments at ambient conditions, the crystal structure of κ -(BEDT-TTF) $_2$ Hg(SCN) $_2$ Br is depicted in Fig. 2 along two crystallographic directions. The BEDT-TTF molecules are all crystallographically equivalent and within the bc plane form dimers according to the κ pattern [25] that are rotated with respect to each other. As seen from Fig. 2(b) the stacking direction b is more pronounced than known from other κ salts leading to a rather isotropic response in our transport and optical measurements. It should be noted that during the electrochemical synthesis, single crystals of the β'' phase tend to grow as well to a considerable size (1–2 mm) [26], and subsequently have to be separated from the desired κ -phase specimens with the help of x-ray or infrared optical inspection.

In the temperature-dependent dc resistivity of κ -(BEDT-TTF) $_2$ Hg(SCN) $_2$ Br displayed in Fig. 1, a sharp metal-insulator transition is identified at $T = 80$ K, confirming the early characterization [23]. While for κ -(BEDT-TTF) $_2$ Hg(SCN) $_2$ Cl

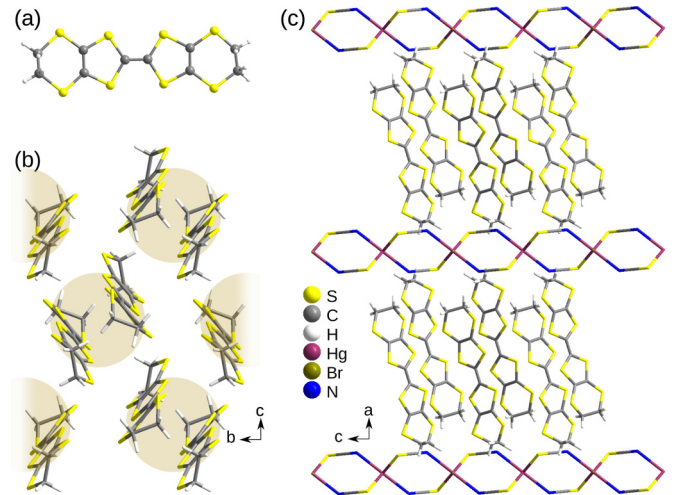


FIG. 2. (a) Sketch of the bis-(ethylenedithio)tetrathiafulvalene molecule, called BEDT-TTF. (b) The view on the BEDT-TTF layers along the out-of-plane a direction illustrates the dimer structure (dimers are denoted by shaded circles). (c) The molecular layers along the conducting bc plane are separated by the $\text{Hg}(\text{SCN})_2\text{Br}^-$ anions. Note that within a dimer the two molecules are displaced along the molecular axis, leading to a reduced transfer integral t_d .

a saturation of $\rho(T)$ is observed at very low temperatures, for the Br analog the slope $|\text{d}\rho(T)/\text{d}T|$ continues to rise as the temperature is lowered. For a more complete study, we have measured the charge transport within the highly conducting (bc) plane, as well as perpendicular to it, using the standard four-probe technique. The sample was slowly cooled (up to 0.5 K/h) from room temperature down to $T = 4$ K using a home-made helium bath cryostat.

In addition, the spectra of the complex dielectric function were obtained from measuring the two-contact complex conductance in the frequency range from 20 Hz to 10 MHz for various temperatures. The Hewlett-Packard 4284A LCR meter and Agilent 4294A impedance analyzer with virtual ground method were used. The capacitive open-loop contribution of the sample holder was always subtracted.

The optical properties of κ -(BEDT-TTF) $_2$ Hg(SCN) $_2$ Br have been investigated by infrared reflectivity measurements from room temperature down to $T = 4$ K for both polarizations along the main axes of the highly conducting (bc) plane. To this end, a Bruker Hyperion infrared microscope was attached to the Fourier-transform spectrometer Bruker IFS 66v/s or Vertex 80v. The sample was cooled down to helium temperatures by a Cryovac Microstat cold-finger cryostat. The far-infrared data were taken by a Bruker IFS 113v equipped with a cold-finger cryostat and *in situ* gold evaporation as reference [27]. In order to perform the Kramers-Kronig analysis, a constant reflectivity extrapolation was used at low frequencies and temperatures $T_{MI} < 80$ K, while a Hagen-Rubens behavior was assumed for elevated temperatures [28]. In addition, the vibrational features were measured perpendicular to the plane ($E \parallel a$) using an infrared microscope. In particular, the *ungerade* C=C vibration $\nu_{27}(\text{b}_{1u})$ of the BEDT-TTF molecules are utilized as a local probe to determine the charge per molecule [27,29–31] and follow any possible charge disproportionation.

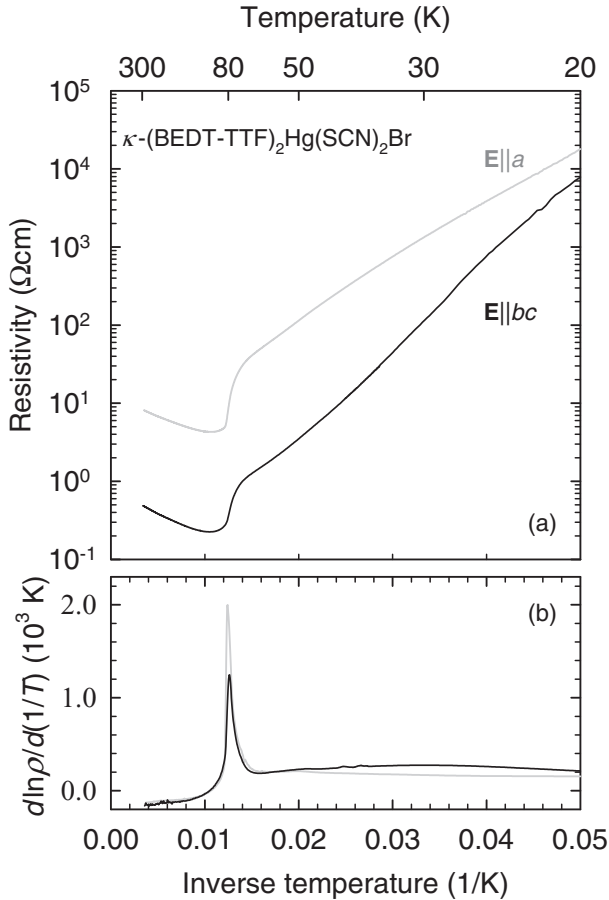


FIG. 3. (a) Electrical resistivity of κ -(BEDT-TTF) $_2$ Hg(SCN) $_2$ Br as a function of inverse temperature measured within the (bc) plane and perpendicular to the plane, i.e., $E \parallel a$. (b) The phase transition around $T_{\text{MI}} \approx 80$ K is identified as the maximum in the derivative.

III. RESULTS AND ANALYSIS

A. Transport properties

In order to gain more information on the transport mechanisms of κ -(BEDT-TTF) $_2$ Hg(SCN) $_2$ Br above and below the phase transition at $T_{\text{MI}} = 80$ K, we have performed dc resistivity measurements along different crystal directions and present the results down to $T = 20$ K in an Arrhenius plot in Fig. 3(a) as a function of inverse temperature. At ambient conditions, the resistivity within the (bc) plane is approximately $0.5 \Omega\text{cm}$ with an anisotropy of less than a factor of 2. Perpendicular to the highly-conducting plane, i.e., parallel to the a axis, ρ_{dc} is about 20 times higher. For all orientations, a very similar temperature dependent metallic resistivity is observed down to 100 K. At T_{MI} , a metal-insulator transition occurs in all three directions with a more or less steep rise in $\rho(T)$ by an order of magnitude or more. It is interesting to note that this temperature-behavior very much resembles the metal-insulator transition observed in other ET-based compounds such as α -(BEDT-TTF) $_2$ I $_3$ and θ -(BEDT-TTF) $_2$ RbZn(SCN) $_4$ [32], where the gap at the density of states rapidly opens at the transition. The insulating state is characterized by an activated behavior $\rho(T) \propto \exp(E_g/2k_B T)$ down to lowest temperatures; no saturation is observed up to

our limit of $10^9 \Omega\text{cm}$. Within the plane ($E \parallel bc$), the activation energy of $E_g/2 = (22 \pm 3)$ meV is basically constant down to $T = 20$ K. In the out-of-plane direction ($E \parallel a$), we extract a similar activation energy of $E_g/2 = (15.5 \pm 2)$ meV, which means it is rather isotropic. If we consider E_g as the full gap in the density of states, the ratio $E_g/k_B T_{\text{MI}} \approx 4-5.6$ is not much higher than 3.53 expected from a conventional mean-field transition. Thus we can consider this system mean-field-like with relatively weak electronic correlations.

B. Dielectric properties

Like in many other charge-ordered (BEDT-TTF) compounds [9,10,33,34], the dielectric properties of κ -(BEDT-TTF) $_2$ Hg(SCN) $_2$ Br can be described by a generalized Debye expression

$$\varepsilon(\omega) - \varepsilon_{\text{HF}} = \frac{\Delta\varepsilon}{1 + (i\omega\tau_0)^{1-\alpha}} \quad (1)$$

at low temperatures, where $\Delta\varepsilon = \varepsilon_0 - \varepsilon_{\text{HF}}$ corresponds to the strength of the dielectric mode; ε_0 and ε_{HF} are the static and high-frequency dielectric constants, respectively; τ_0 is the mean relaxation time; and $1 - \alpha$ is the symmetric broadening of the relaxation time distribution. The temperature dependencies of the extracted parameters $\Delta\varepsilon$, $1 - \alpha$, and τ_0 are plotted in Fig. 4 as a function of inverse temperature $1/T$. The dielectric relaxation can be detected only at temperatures below 60 K. Above $T \approx 35$ K, we can determine only the dielectric relaxation strength by measuring the capacitance at 1 MHz. At first glance the relaxation appears rather broad. The dielectric strength perpendicular to planes ($E \parallel a$) is only of the order of 10 and less while the strength of the dielectric response $E \parallel bc$ is on the order of 100 (not shown), which mirrors the similarly weak anisotropy found in dc data. Most important, for both orientations the intensity of the modes becomes smaller by about an order of magnitude as the temperature is reduced to 10 K; these findings are in contrast to the behavior commonly observed in low-dimensional organic charge transfer salts [32]. It clearly indicates that κ -(BEDT-TTF) $_2$ Hg(SCN) $_2$ Br does not exhibit indications of charge order and shows only very weak relaxorlike properties, further underlining the absence of strong electronic correlations.

For both orientations, the temperature behavior of $\tau_0(T)$ shows no saturation and basically follows an Arrhenius law between 40 and 12 K, as plotted in Fig. 4(c). The activation energy is comparable with the dc resistivity. This indicates that electronic screening by quasifree charge carriers is the dominant relaxation mechanism.

Around $T \approx 20-30$ K, we find the most pronounced change in the dielectric behavior that can be seen even better by directly looking at the temperature dependence of the dielectric constant. In Fig. 5, we present $\varepsilon'(T)$ measured at different frequencies for the orientations parallel and perpendicular to the (bc) plane. A clear step can be seen around $T = 20$ K that becomes more pronounced as the frequency increases to 1 MHz. This is accompanied by a change in $1 - \alpha$ and $\Delta\varepsilon$ at the same temperatures in Fig. 4, which suggests the entities responsible for the dielectric response are not correlated as temperature is lowered.

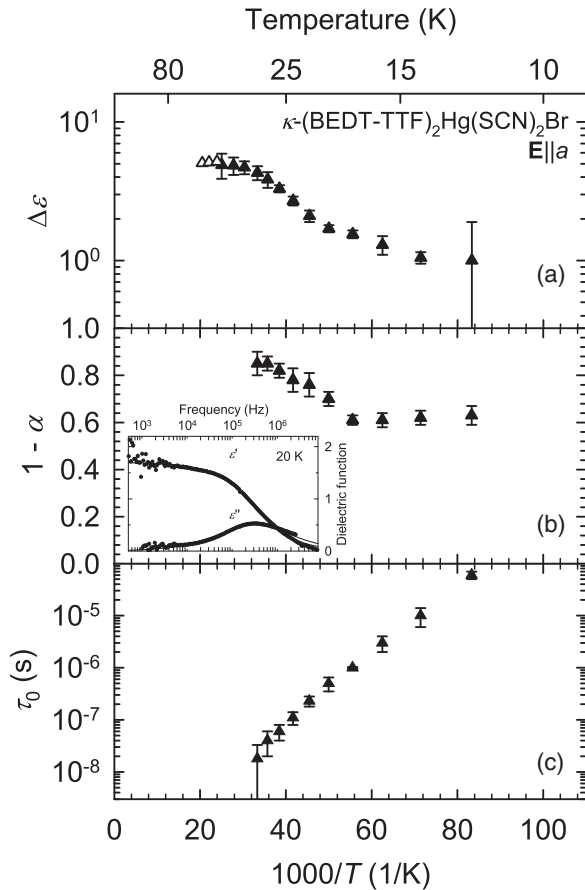


FIG. 4. (a) Dielectric strength $\Delta\epsilon$, (b) distribution width of relaxation times $1 - \alpha$, and (c) mean relaxation time τ_0 of κ -(BEDT-TTF) $_2$ Hg(SCN) $_2$ Br as a function of inverse temperature measured perpendicular to the (bc) plane. (Inset) Real and imaginary parts of the measured dielectric response (points) and fit (lines, see text) at a select temperature.

C. Infrared-active molecular vibrations

Microscopic information on the charge distribution and its temperature behavior can be obtained by optical spectroscopy. To this end, we performed infrared reflectance measurements for the polarization perpendicular to the layers, i.e., $E \parallel a$. In

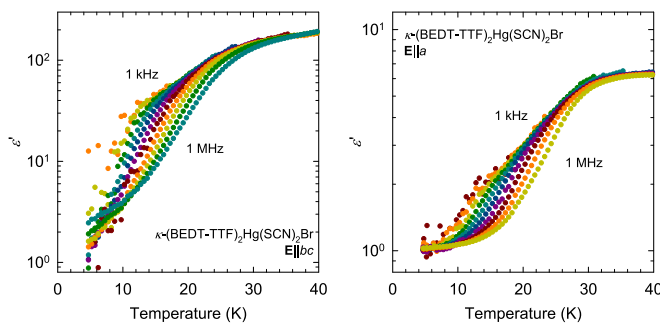


FIG. 5. Real part of the dielectric constant $\epsilon'(T)$ of κ -(BEDT-TTF) $_2$ Hg(SCN) $_2$ Br determined (left panel) within the (bc) plane and (right panel) for $E \parallel a$ (perpendicular to the plane) at various frequencies from 1 kHz up to 1 MHz as indicated. Note the logarithmic scale.

this orientation, the optical response resembles an insulator with low reflectivity and correspondingly low values of conductivity, in agreement with the quasi-two-dimensional character of these materials, deduced from the dc conductivity presented in Fig. 3.

Of primary interest, however, are the superimposed infrared-active vibrational features of the BEDT-TTF molecule and lattice. The out-of-phase molecular vibrations of the two C=C bonds of the inner rings provide a powerful and well-established method to identify the amount of charge on molecular lattice sites [27,29,31]. The frequency dependence of the $\nu_{27}(b_{1u})$ mode allows for a quantitative determination of the charge per BEDT-TTF molecule and thus the most accurate way to monitor the temperature-dependence of the charge disproportionation.

The resulting conductivity spectra in the region of the $\nu_{27}(b_{1u})$ mode are presented in Fig. 6 for κ -(BEDT-TTF) $_2$ Hg(SCN) $_2$ Br in comparison with spectra of the Cl analog. κ -(BEDT-TTF) $_2$ Hg(SCN) $_2$ Cl is known [16] to undergo a charge-order transition around $T_{CO} = 30$ K, as can be clearly seen from the splitting of the $\nu_{27}(b_{1u})$ vibration, which peaks around 1455 cm^{-1} at room temperature and narrows on cooling down. A higher-frequency shoulder can be identified that becomes more pronounced at low temperatures; this double feature indicates the two crystallographically different sites per unit cell. For a quantitative analysis, we fit the bands by two Fano resonances for $T > 30$ K and four modes below T_{CO} ; the results are plotted in the inset and perfectly agree with our previous observations [16] where we concluded a charge difference of $2\delta\rho = 0.2e$ between two different molecular sites. Löhle *et al.* studied the pressure dependence of the charge ordered phase [17] and found a rapid suppression of T_{CO} by about 0.7 kbar and the absence of charge disproportionation for $p > 4$ kbar.

For the present case of κ -(BEDT-TTF) $_2$ Hg(SCN) $_2$ Br, nothing like that is observed in the lower panel of Fig. 6. At room temperature the broad $\nu_{27}(b_{1u})$ feature occurs at 1457 cm^{-1} with a comparable width and temperature dependence down to $T \approx 100$ K. No drastic change is observed when the sample is cooled further below T_{MI} , in a way similar to Cu-based κ -BEDT-TTF $_2X$ systems [8]. At the lowest temperature, the double peak structure around 1460 cm^{-1} has slightly changed in so far as the higher-frequency peak is more pronounced. In addition, a second feature develops at 1445 cm^{-1} at below temperatures as high as 150 K, meaning it is not related to the metal-insulator transition. Even though it is tempting to ascribe its temperature evolution to the establishing of the low-temperature phase, it appears to be governed by thermal broadening: the width and strength behave in a manner similar to the dominant 1460 cm^{-1} peak as well as the normal-phase $\nu_{27}(b_{1u})$ peak of the κ -(BEDT-TTF) $_2$ Hg(SCN) $_2$ Cl analog.

It is interesting to note that the ν_{27} mode observed in κ -(BEDT-TTF) $_2$ Hg(SCN) $_2$ Br is much broader than in the Cl analog and comparable to the ones found in the spin-liquid candidates κ -(BEDT-TTF) $_2$ Cu $_2$ (CN) $_3$ and κ -(BEDT-TTF) $_2$ Ag $_2$ (CN) $_3$ [8,34], where charge inhomogeneities or fluctuations might be of relevance [32,34]. These findings provide evidence that the metal-insulator transition observed

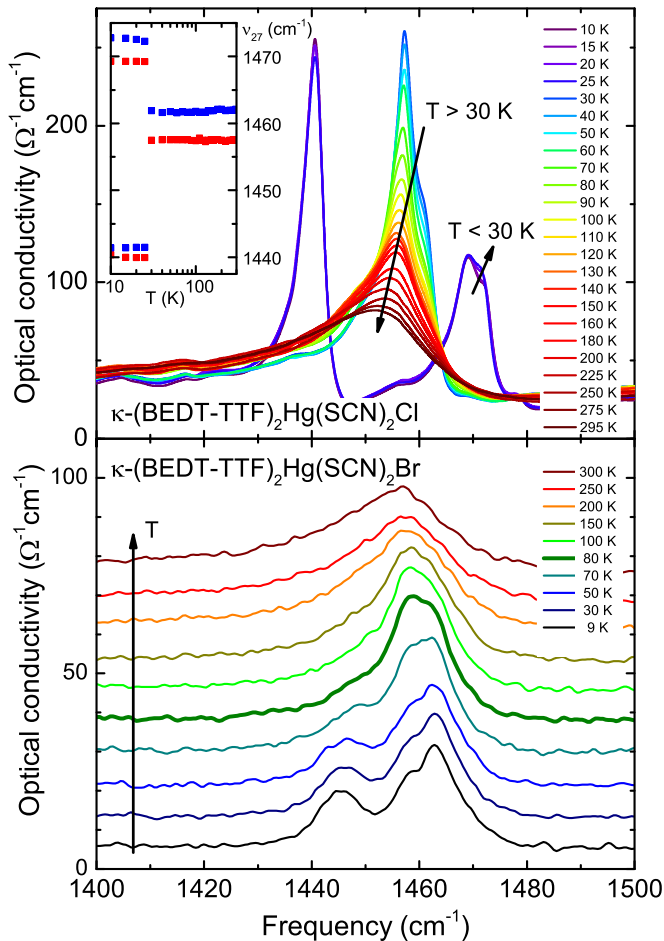


FIG. 6. Temperature dependence of the absorption feature related to the molecular vibration $\nu_{27}(b_{1u})$, which is seen as a local probe of the charge per BEDT-TTF molecule. In the upper panel, a clear splitting is observed in κ -(BEDT-TTF) $_2$ Hg(SCN) $_2$ Cl as the temperature is reduced below the charge order transition $T_{CO} = 34$ K. The inset displays the peak frequency as a function of temperature. The lower panel shows the ν_{27} vibrational mode of κ -(BEDT-TTF) $_2$ Hg(SCN) $_2$ Br for different temperature in a waterfall plot, i.e., the curves are shifted with respect to each other. Except of a gradual development of a side peak, no splitting due to charge order is found.

in κ -(BEDT-TTF) $_2$ Hg(SCN) $_2$ Br at 80 K is not due to static charge ordering. Recent measurements of the Raman spectra as a function of temperature support this conclusion: no indications of charge imbalance has been observed [35] as the metal-insulator transition is passed.

D. In-Plane infrared properties

The electrodynamic properties of κ -(BEDT-TTF) $_2$ Hg(SCN) $_2$ Br were investigated by measuring the reflectivity at different temperatures for $4 \text{ K} \leq T < 300 \text{ K}$; in Fig. 7, we plot $R(\omega)$ for the two polarizations $E \parallel c$ and $E \parallel b$ together with the optical conductivity obtained by the Kramers-Kronig relations. The quasi-two-dimensional conductor displays a rather weak anisotropy in its optical response, very similar to its Cl analog κ -(BEDT-TTF) $_2$ Hg(SCN) $_2$ Cl and to κ -(BEDT-TTF) salts

with Cu-containing anions. From the crystal structure [Fig. 2(b)] we can identify the b axis as preferred stacking direction of the BEDT-TTF molecules.

Most obvious, the mid-infrared band is more intense along the b direction [Figs. 7(c) and 7(d)], leading to a drop in $R(\omega)$ around 3500 cm^{-1} that resembles the plasma edge of regular metals. We associate this optical anisotropy to the arrangement of the BEDT-TTF dimers as depicted in Fig. 2(b): the intradimer charge transfer is in particular excited by $E \parallel b$. The low-frequency reflectivity is rather small, between 0.4 and 0.6. Only when cooled down to $T = 100 \text{ K}$ a pronounced Hagen-Rubens behavior is measured. This corresponds to the increase in conductivity by a factor of 3 to 4 (see insets of Fig. 7), in good agreement with the metallic temperature dependence seen in dc resistivity (Figs. 1 and 3) above the metal-to-insulator transition.

From the mid-infrared conduction band we can extract the electronic parameters [27,36–38], in particular, the maximum ν_{\max} is proportional to the Coulomb repulsion U . At $T = 100 \text{ K}$ we find approximately 2200 cm^{-1} for $E \parallel c$, while for $E \parallel b$ it is only 1950 cm^{-1} . In both cases, the values increase by about 10% as the temperature rises to room temperature. The overall behavior is similar to the observations reported for κ -(BEDT-TTF) $_2$ Hg(SCN) $_2$ Cl, however, the absolute values are reduced, indicating smaller effect of electronic correlations.

We describe the zero-frequency contributions by a Drude-like conductivity. In accord to the dc data, the spectral weight $\int \sigma(\omega) d\omega = \omega_p/8$ obtained for both directions differs by a factor of 2, independent on temperature. For most-conducting direction ($E \parallel b$), the plasma frequency $\omega_p/(2\pi c) = 1500 \text{ cm}^{-1}$ at ambient temperature increases to 4000 cm^{-1} at $T = 100 \text{ K}$. Here the width increases by a slightly more than a factor of 2 when the temperature is reduced to T_{MI} . Within the uncertainty, no change is observed along the c direction.

For κ -(BEDT-TTF) $_2$ Hg(SCN) $_2$ Br, we observe a larger spectral weight of the Drude component compared to the one extracted for the Cl analog, corroborating our conclusion drawn above from the mid-infrared band, that the title compound is less-correlated than κ -(BEDT-TTF) $_2$ Hg(SCN) $_2$ Cl. A similar order was observed for the copper-based salts, as κ -(BEDT-TTF) $_2$ Cu[N(CN) $_2$ Cl] is a Mott insulator, while the Br analog becomes superconducting.

For $T < T_{MI}$, the low-frequency reflectivity drops significantly in both polarizations. Although strong phonon bands around 200 – 450 cm^{-1} cause considerable intensity in $\sigma_1(\omega)$ even at $T = 4 \text{ K}$, we might identify an isotropic gap around 500 cm^{-1} for both directions. Within experimental errors, this value agrees nicely with the transport gap extracted from dc data. Additionally, we note that frequencies up to 1000 cm^{-1} the optical conductivity decreases when cooling from 70 to 4 K, which indicates a sort of soft gap behavior. Accordingly, the spectral weight is shifted to the mid-infrared band, which grows considerably.

IV. DISCUSSION

By now it is well established that κ -(BEDT-TTF) $_2$ Hg(SCN) $_2$ Cl undergoes a metal-insulator transition due to charge ordering at $T_{CO} = 30 \text{ K}$: the resistivity $\rho_{dc}(T)$

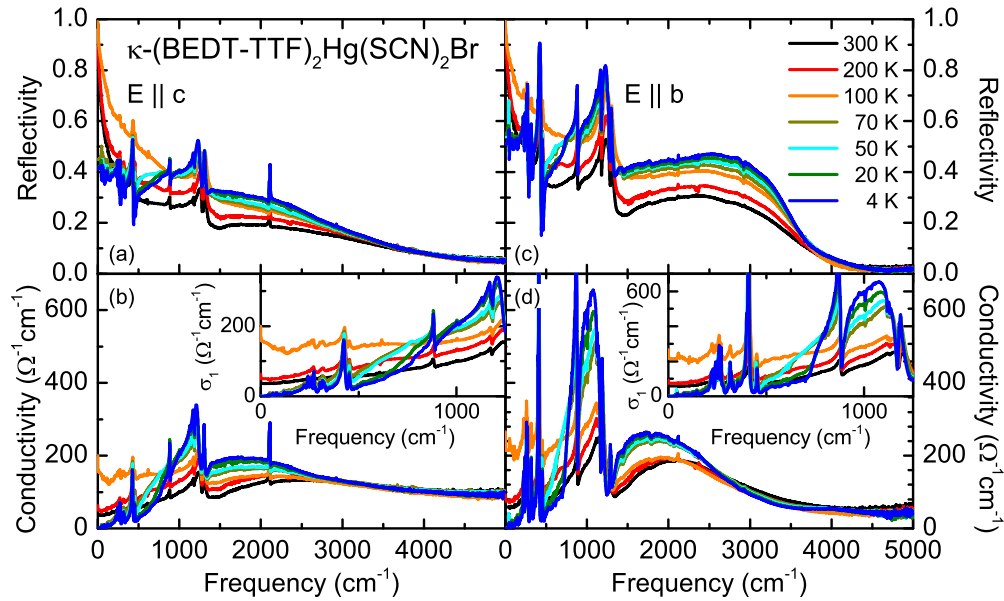


FIG. 7. Optical reflectivity of κ -(BEDT-TTF) $_2$ Hg(SCN) $_2$ Br measured at different temperatures as indicated (a) for light polarized along the c direction and (c) for $E \parallel b$. [(b) and (d)] The corresponding optical conductivity as obtained by Kramers-Kronig analysis for the two different orientations. The insets show the low-frequency conductivity $\sigma_1(\omega)$ on an enlarged scale.

continuously rises by orders of magnitude (Fig. 1) and the charge-sensitive vibrational $\nu_{27}(b_{1u})$ mode splits (Fig. 6) indicating a charge disproportionation $2\delta_\rho = 0.2e$ at low temperatures. In contrast, no clear splitting of the $\nu_{27}(b_{1u})$ mode is observed in the sibling κ -(BEDT-TTF) $_2$ Hg(SCN) $_2$ Br, ruling out any significant charge disproportionation. Hence, κ -(BEDT-TTF) $_2$ Hg(SCN) $_2$ Br does not enter a charge-ordered ground state.

Applying minor pressure, the Mott insulator with Cu-based anions κ -(BEDT-TTF) $_2$ Cu[N(CN) $_2$ Cl] turns metallic and superconducting, very much like κ -(BEDT-TTF) $_2$ Cu[N(CN) $_2$ Br] at ambient pressure. In the case of the Hg-based κ -(BEDT-TTF) $_2$ Hg(SCN) $_2$ Cl, the relation to the Br analog is rather different: pressure rapidly suppresses the charge-ordered state in κ -(BEDT-TTF) $_2$ Hg(SCN) $_2$ Cl, which becomes metallic at all temperatures [17]. This is in striking contrast to κ -(BEDT-TTF) $_2$ Hg(SCN) $_2$ Br, which shows no charge ordering but still features a metal-insulator transition of a different kind.

It has been suggested [4] that charge fluctuations within the dimers may couple to neighboring entities; and in particular in the frustrated case of a triangular lattice it may give rise to the spin liquid state. Pressure enhances the interdimer interaction and may explain why κ -(BEDT-TTF) $_2$ Hg(SCN) $_2$ Cl exhibits a strong and static charge order, while only charge fluctuations may be present in κ -(BEDT-TTF) $_2$ Hg(SCN) $_2$ Br.

For the organic Mott insulators κ -(BEDT-TTF) $_2$ Cu[N(CN) $_2$ Cl] and κ -(BEDT-TTF) $_2$ Cu $_2$ (CN) $_3$, the temperature evolution of dielectric spectra resembles relaxor ferroelectrics [9,10,39,40]. In the case of κ -(BEDT-TTF) $_2$ Hg(SCN) $_2$ Cl, the behavior is similar to other charge-ordered compounds, such as α -(BEDT-TTF) $_2$ I $_3$ [33,41], where two dielectric relaxation modes appeared in the kilohertz-megahertz frequency range. Nothing like that however is observed in κ -(BEDT-TTF) $_2$ Hg(SCN) $_2$ Br,

supporting our conclusion that the compound is not a charge-order insulator, but also that it is not clear whether the disorder in the molecular and anion layers is an issue here. The temperature-dependence of the dielectric parameters indicate some relaxational behavior screened by the conduction electrons remaining below the phase transition. It is 30 times more pronounced within the (bc) plane compared to the perpendicular direction. Below 30 K the mode vanishes rapidly and is basically absent at $T = 10$ K, although in this temperature range no additional transition can be identified in the transport or optical properties. It might be tempting to attribute the dielectric response to dipolar fluctuations [32], forming a kind of non-Barrett quantum electric-dipole liquid [42]. Since pure dipolar coupling does not cause frustration in a two-dimensional triangular lattice, the transfer integrals are significant and do increase when going from κ -(BEDT-TTF) $_2$ Hg(SCN) $_2$ Br to the Cl analog.

The low-temperature optical conductivity of κ -(BEDT-TTF) $_2$ Hg(SCN) $_2$ Br exhibits a shape similar to the room-temperature spectra of other κ -(BEDT-TTF) salts, such as κ -(BEDT-TTF) $_2$ Cu[N(CN) $_2$ Cl], with a gap at low frequencies, strong electron-molecular vibrational (emv) coupled features, and a band at about 2000 cm^{-1} . The electronic properties of these compounds can be well described by assuming a lattice of dimers with one electron per site. The simple Hubbard model of a half-filled system describes the main physics rather well. In comparison to κ -(BEDT-TTF) $_2$ Hg(SCN) $_2$ Cl and κ -(BEDT-TTF) $_2$ Cu[N(CN) $_2$ Cl], the effect of electronic correlations seems to be less important in κ -(BEDT-TTF) $_2$ Hg(SCN) $_2$ Br. This is concluded from the mean-field-like dc transport and maximum of the mid-infrared conductivity band, but also from the spectral weight of the Drude component (Fig. 7). The zero-frequency peak is higher than typically observed in the Cu family and it shows up at high temperatures, as a result of smaller Hubbard on-site repulsion U [37,38].

With the metal-insulator transition prominently at 80 K, we do not observe a gradual increase in resistivity of κ -(BEDT-TTF)₂Hg(SCN)₂Br (Fig. 1) as known from the dimerized Mott insulators κ -(BEDT-TTF)₂X with Cu ions in the anion layers, such as κ -(BEDT-TTF)₂Cu[N(CN)₂Cl] or κ -(BEDT-TTF)₂Cu₂(CN)₃ [8]. This leads us to conclude that the $T = 80$ K transition is not a regular Mott transition. This is supported by the analysis of our optical data and structural considerations. The rapid change in resistivity must therefore have other reasons, most likely some subtle magnetic ordering. In this regard, it is of interest to recall ESR investigations by Yudanova *et al.*, who measured hydrogenated and deuterated κ -(BEDT-TTF)₂Hg(SCN)₂Br and κ -(BEDT-TTF)₂Hg(SCN)₂Cl down to low temperature [43]. After subtracting a Curie contribution, the spin susceptibility vanishes at the metal-insulator transition, following $\chi(T) = C/T \exp(-\Delta/T)$, with $\Delta \approx 500$ K, which agrees nicely with the charge gap extracted from our optical and dc transport data. They conclude a first-order structural phase transition with a considerable localization of the electrons on the BEDT-TTF molecules. Recent low-temperature x-ray diffraction studies, however, did not reveal any evidence of a unit cell doubling or other structural changes in κ -(BEDT-TTF)₂Hg(SCN)₂Br. Thus we cannot explain the change in transport and magnetic properties by a change in the crystal structure. Comprehensive investigations of magnetic properties are on its way in order to clarify the magnetic ground state of κ -(BEDT-TTF)₂Hg(SCN)₂Br as well as the Cl analog. Additionally, conventional density-wave instabilities are excluded by the

absence of structural changes as seen by x-ray and infrared vibrations. Future low-temperature x-ray experiments are needed to explore if subtler structural effects play a role in the fluctuating charge present in this compound.

V. CONCLUSIONS AND OUTLOOK

From our comprehensive transport, dielectric and optical investigations of the dimerized organic charge transfer salt κ -(BEDT-TTF)₂Hg(SCN)₂Br, we can rule out that the metal-insulator transition at $T = 80$ K is due to a charge ordering. No pronounced structural change takes place as well. We can estimate the effective correlations to be weaker compared to the κ -(BEDT-TTF) salts containing Cu-based anions. The system is also more metallic than the sister compound κ -(BEDT-TTF)₂Hg(SCN)₂Cl. Although electronic correlations do play a decisive role, the phase below the 80-K transition cannot be explained as a simple Mott insulator. We suggest that magnetic fluctuations might play an important role in supporting charge fluctuations revealed by our infrared vibrational spectra.

ACKNOWLEDGMENTS

We do acknowledge valuable discussion with N. Drichko and A. Pustogow. The project was supported by the Deutsche Forschungsgemeinschaft (DFG) by DR228/39-1 and DR228/52-1, the Deutsche Akademischer Austauschdienst (DAAD), as well as the Croatian Science Foundation project IP-2013-11-1011.

-
- [1] T. Ishiguro, K. Yamaji, and G. Saito, *Organic Superconductors*, 2nd ed. (Springer-Verlag, Berlin, 1998); N. Toyota, M. Lang, and J. Müller, *Low-Dimensional Molecular Metals* (Springer-Verlag, Berlin, 2007).
- [2] K. Kanoda and R. Kato, *Annu. Rev. Condens. Matter Phys.* **2**, 167 (2011).
- [3] B. J. Powell and R. H. McKenzie, *Rep. Prog. Phys.* **74**, 056501 (2011).
- [4] C. Hotta, *J. Phys. Soc. Jpn.* **72**, 840 (2003); *Phys. Rev. B* **82**, 241104 (2010); *Crystals* **2**, 1155 (2012).
- [5] M. Naka and S. Ishihara, *J. Phys. Soc. Jpn.* **79**, 063707 (2010).
- [6] H. Gomi, T. Imai, A. Takahashi, and M. Aihara, *Phys. Rev. B* **82**, 035101 (2010).
- [7] H. Li, R. T. Clay, and S. Mazumdar, *J. Phys.: Condens. Matter* **22**, 272201 (2010); S. Dayal, R. T. Clay, H. Li, and S. Mazumdar, *Phys. Rev. B* **83**, 245106 (2011); R. T. Clay, S. Dayal, H. Li, and S. Mazumdar, *Phys. Status Solidi B* **249**, 991 (2012).
- [8] K. Sedlmeier, S. Elsässer, D. Neubauer, R. Beyer, D. Wu, T. Ivek, S. Tomić, J. A. Schlueter, and M. Dressel, *Phys. Rev. B* **86**, 245103 (2012).
- [9] S. Tomić, M. Pinterić, T. Ivek, K. Sedlmeier, R. Beyer, D. Wu, J. A. Schlueter, D. Schweitzer, and M. Dressel, *J. Phys.: Condens. Matter* **25**, 436004 (2013).
- [10] M. Pinterić, M. Čulo, O. Milat, M. Basletić, B. Korin-Hamzić, E. Tafra, A. Hamzić, T. Ivek, T. Peterseim, K. Miyagawa, K. Kanoda, J. A. Schlueter, M. Dressel, and S. Tomić, *Phys. Rev. B* **90**, 195139 (2014); M. Pinterić, T. Ivek, M. Čulo, O. Milat, M. Basletić, B. Korin-Hamzić, E. Tafra, A. Hamzić, M. Dressel, and S. Tomić, *Physica B* **460**, 202 (2015).
- [11] Y. Shimizu, K. Miyagawa, K. Kanoda, M. Maesato, and G. Saito, *Phys. Rev. B* **73**, 140407 (2006); K. Kanoda (private communication).
- [12] K. Yakushi, K. Yamamoto, T. Yamamoto, Y. Saito, and A. Kawamoto, *J. Phys. Soc. Jpn.* **84**, 084711 (2015).
- [13] M. Dressel, P. Lazić, A. Pustogow, E. Zhukova, B. Gorshunov, J. A. Schlueter, O. Milat, B. Gumhalter, and S. Tomić, *Phys. Rev. B* **93**, 081201 (2016).
- [14] M.-L. Doublet, E. Canadell, and R. P. Shibaeva, *J. Phys. I (France)* **4**, 1479 (1994); P. Le Maguerès, L. Ouahab, N. Conan, C. J. Gomez-García, P. Delhaés, J. Even, and M. Bertault, *Solid State Commun.* **97**, 27 (1996); L. Ouahab, S. Golhen, T. Le Hoerff, J. Guillevic, L. Tual, N. Hérou, J. Amiell, P. Delhaès, K. Binet, and J. M. Fabre, *Synth. Met.* **102**, 1642 (1999); R. Świetlik, A. Łapiński, L. Ouahab, and K. Yakushi, *Comptes Rendus Chimie* **6**, 395 (2003); R. Świetlik, A. Łapiński, M. Polomska, L. Ouahab, and J. Guillevic, *Synth. Met.* **133**, 273 (2003); R. Świetlik, L. Ouahab, J. Guillevic, and K. Yakushi, *Macromolecular Symposia* **212**, 219 (2004); R. Świetlik, A. Łapiński, M. Polomska, L. Ouahab, and A. Ota, *J. Low Temp. Phys.* **142**, 641 (2006); A. Ota, L. Ouahab, S. Golhen, Y. Yoshida, M. Maesto, G. Saito, and R. Świetlik, *Chem. Mater.* **19**, 2455 (2007).

- [15] S. Yasin, E. Rose, M. Dumm, N. Drichko, M. Dressel, J. A. Schlueter, E. I. Zhilyaeva, S. Torunova, and R. N. Lyubovskaya, *Physica B* **407**, 1689 (2012).
- [16] N. Drichko, R. Beyer, E. Rose, M. Dressel, J. A. Schlueter, S. A. Torunova, E. I. Zhilyaeva, and R. N. Lyubovskaya, *Phys. Rev. B* **89**, 075133 (2014).
- [17] A. Löhle, E. Rose, S. Singh, R. Beyer, E. Tafra, T. Ivek, E. I. Zhilyaeva, R. N. Lyubovskaya, and M. Dressel, *J. Phys.: Condens. Matter* **29**, 055601 (2017).
- [18] M. Dressel, G. Grüner, J. P. Pouget, A. Breining, and D. Schweitzer, *J. Phys. (France) I* **4**, 579 (1994).
- [19] R. Beyer, A. Dengl, T. Peterseim, S. Wackerow, T. Ivek, A. V. Pronin, D. Schweitzer, and M. Dressel, *Phys. Rev. B* **93**, 195116 (2016).
- [20] R. B. Lyubovskii, R. N. Lyubovskaya, and O. A. Dyachenko, *J. Phys. I (France)* **6**, 1609 (1996).
- [21] H. Jeschke and R. Valenti (private communication).
- [22] H. Seo, C. Hotta, and H. Fukuyama, *Chem. Rev.* **104**, 5005 (2004); H. Seo, J. Merino, H. Yoshioka, and M. Ogata, *J. Phys. Soc. Jpn.* **75**, 051009 (2006).
- [23] M. Z. Aldoshina, R. N. Lyubovskaya, S. V. Konovalikhin, O. A. Dyachenko, G. V. Shilov, M. K. Makova, and R. B. Lyubovskii, *Synth. Met.* **56**, 1905 (1993).
- [24] S. V. Konovalikhin, G. V. Shilov, O. A. D'yachenko, R. N. Lyubovskaya, M. Z. Aldoshina, and R. B. Lyubovskii, *Russ. Chem. Bull.* **41**, 704 (1992).
- [25] T. Mori, H. Mori, and S. Tanaka, *Bull. Chem. Soc. Jpn.* **72**, 179 (1999).
- [26] W. Li, E. Rose, M. V. Tran, R. Hübner, A. Łapiński, R. Świetlik, S. A. Torunova, E. I. Zhilyaeva, R. N. Lyubovskaya, and M. Dressel, *J. Chem. Phys.*, doi:10.1063/1.4997198.
- [27] M. Dressel and N. Drichko, *Chem. Rev.* **104**, 5689 (2004).
- [28] M. Dressel and G. Grüner, *Electrodynamics of Solids* (Cambridge University Press, Cambridge, 2002).
- [29] N. Drichko, S. Kaiser, Y. Sun, C. Clauss, M. Dressel, H. Mori, J. Schlueter, E. I. Zhilyaeva, S. A. Torunova, and R. N. Lyubovskaya, *Physica B* **404**, 490 (2009).
- [30] T. Yamamoto, M. Uruichi, K. Yamamoto, K. Yakushi, A. Kawamoto, and H. Taniguchi, *J. Phys. Chem. B* **109**, 15226 (2005).
- [31] A. Girlando, *J. Phys. Chem. C* **115**, 19371 (2011).
- [32] S. Tomić and M. Dressel, *Rep. Prog. Phys.* **78**, 096501 (2015).
- [33] T. Ivek, B. Korin-Hamzić, O. Milat, S. Tomić, C. Clauss, N. Drichko, D. Schweitzer, and M. Dressel, *Phys. Rev. Lett.* **104**, 206406 (2010); *Phys. Rev. B* **83**, 165128 (2011).
- [34] M. Pinterić, P. Lazić, A. Pustogow, T. Ivek, M. Kuveždić, O. Milat, B. Gumhalter, M. Basletić, M. Čulo, B. Korin-Hamzić, A. Löhle, R. Hübner, M. Sanz Alonso, T. Hiramatsu, Y. Yoshida, G. Saito, M. Dressel, and S. Tomić, *Phys. Rev. B* **94**, 161105 (2016).
- [35] N. Hassan, S. Cunningham, M. Mourigal, E. I. Zhilyaeva, S. A. Torunova, R. N. Lyubovskaya, and N. Drichko, [arXiv:1704.04482](https://arxiv.org/abs/1704.04482).
- [36] D. Faltermeier, J. Barz, M. Dumm, M. Dressel, N. Drichko, B. Petrov, V. Semkin, R. Vlasova, C. Mézière, and P. Batail, *Phys. Rev. B* **76**, 165113 (2007).
- [37] J. Merino, M. Dumm, N. Drichko, M. Dressel, and R. H. McKenzie, *Phys. Rev. Lett.* **100**, 086404 (2008).
- [38] M. Dumm, D. Faltermeier, N. Drichko, M. Dressel, C. Mézière, and P. Batail, *Phys. Rev. B* **79**, 195106 (2009).
- [39] M. Abdel-Jawad, I. Terasaki, T. Sasaki, N. Yoneyama, N. Kobayashi, Y. Uesu, and C. Hotta, *Phys. Rev. B* **82**, 125119 (2010).
- [40] P. Lunkenheimer, J. Müller, S. Krohns, F. Schrettle, A. Loidl, B. Hartmann, R. Rommel, M. de Souza, J. A. Schlueter, and M. Lang, *Nat. Mater.* **11**, 755 (2012).
- [41] T. Ivek, M. Čulo, M. Kuveždić, E. Tutiš, M. Basletić, B. Mihaljević, E. Tafra, S. Tomić, A. Löhle, M. Dressel, D. Schweitzer, and B. Korin-Hamzić, [arXiv:1703.06055](https://arxiv.org/abs/1703.06055).
- [42] S.-P. Shen, J.-C. Wu, J.-D. Song, X.-F. Sun, Y.-F. Yang, Y.-S. Chai, D.-S. Shang, S.-G. Wang, J. F. Scott, and Y. Sun, *Nat. Commun.* **7**, 10569 (2016).
- [43] E. I. Yudanov, S. K. Hoffmann, A. Graja, and R. N. Lyubovskaya, *Synth. Met.* **66**, 43 (1994); E. I. Yudanov, R. N. Lyubovskaya, S. K. Hoffmann, and A. Graja, *ibid.* **70**, 971 (1995); E. I. Yudanov, S. K. Hoffmann, A. Graja, S. V. Konovalikhin, O. A. Dyachenko, R. B. Lyubovskii, and R. N. Lyubovskaya, *ibid.* **73**, 227 (1995); E. I. Yudanov, R. N. Lyubovskaya, S. V. Konovalikhin, and O. A. Dyachenko, *ibid.* **86**, 2195 (1997).